American Mineralogist, Volume 80, pages 1166–1173, 1995

# Annealing of synthetic hammarite, $Cu_2Pb_2Bi_4S_9$, and the nature of cation-ordering processes in the bismuthinite-aikinite series

ALLAN PRING
Department of Mineralogy, South Australian Museum, North Terrace, Adelaide, South Australia 5000, Australia

## ABSTRACT

The progress of ordering of $Cu^+$ and $Pb^{2+}$ in synthetic hammarite, $Cu_2Pb_2Bi_4S_9$, has been monitored by the form and sharpness of satellite reflections in electron diffraction patterns and by high-resolution transmission electron microscopy (HRTEM). The initial state of the synthetic hammarite is that of the parent bismuthinite cell, with a disordered distribution of Bi and Pb on the M2 sites and Cu disordered over the available tetrahedral sites with two-thirds occupancy. Strong superlattice reflections, corresponding to a supercell of the bismuthinite parent with a $3a$ period, were observed in samples annealed at 175 and 225 °C for 24 months or longer, and HRTEM images show crystals with domains of a well-ordered $3a$ supercell phase. In addition to the $3a$ supercell, superlattices with a $5a$ period were also observed in some crystal fragments, indicating chemical variation within the annealed products. HRTEM was used to monitor Cu ordering and revealed that the distribution of Cu and Pb in the cell is not that of hammarite but of a lower symmetry supercell consisting of the intergrowth of one aikinite cell (two aikinite units) with two krupkaite cells (four krupkaite units). Fully ordered natural hammarite has a $3a$ supercell of the bismuthite parent, but with the two aikinite units and four krupkaite units ordered into a centrosymmetric structure in *Pbnm*. The lattice images show steps in ordering; cations order first on a local scale to create end-member polysome strips, then the polysome strips order to form simple supercells, and finally, with longer annealing time, the Pb and Cu are reordered into the higher symmetry hammarite cell. The electron diffraction and high-resolution lattice image data suggest that the ordering of $Cu^+$ and $Pb^{2+}$ in these minerals is coupled and that $Pb^{2+}$ does not order before $Cu^+$. The results of these annealing experiments indicate that in nature intermediate compositions in the bismuthinite-aikinite series consist of compositionally well-ordered polysome strips, which, depending on the initial composition and the cooling rate, may remain as disordered intergrowths (stacking disorder), form ordered intergrowths, or fully order into the supercell minerals.

## INTRODUCTION

The bismuthinite-aikinite group is a polysomatic series of minerals that lie on the composition line between $Bi_2S_3$ and $CuPbBiS_3$. They are found in a wide variety of ore deposits, particularly in hydrothermal vein systems, but in general they are not common minerals. The series contains six well-ordered minerals intermediate in composition between the end-members bismuthinite, $Bi_2S_3$, and aikinite, $CuPbBiS_3$. The bismuthinite structure can be considered the archetype for the series, with the other members being derived from it by the ordered substitution of Pb for Bi coupled with the insertion of Cu into a tetrahedral site. The bismuthinite structure, in the centric space group *Pbnm*, consists of quadruple $Bi_4S_6$ units, in which half the Bi is nominally threefold coordinated (M1 site) and the other half is nominally fivefold coordinated (M2 site), there being two such units per unit cell (Fig. 1). The structure can also be visualized in terms of trigonal prisms: the M1 site has three short bonds and three longer contacts, and the M2 site is a monocapped trigonal prism with five short bonds and two longer contacts. All atoms in the unit cell lie on a mirror plane at either ¼ or ¾$c$, and the height of trigonal prisms (3.91 Å) defines $c$ (Fig. 1). Krupkaite is derived from bismuthinite by replacing one-half of the $Bi^{3+}$ with $Pb^{2+}$ in the M2 site and inserting $Cu^+$ into one-half of the available tetrahedral sites in an ordered fashion. This ordering results in a lowering in symmetry from *Pbnm* to the acentric group $Pb2_1m$. In aikinite the M2 site is fully occupied by $Pb^{2+}$, $Cu^+$ occupies all four tetrahedral sites, and the symmetry is again *Pbnm*. In the structure refinements of aikinite and krupkaite, there is no evidence of Pb entering the M1 site; it is restricted to the M2 site (Mumme, 1975; Kohatsu and Wuensch, 1971; Ohmasa and Nowacki, 1970).

In addition to the end-members, bismuthinite (B) and aikinite (A), and the mid-member krupkaite (K), which all have simple cells based on the archetype, minerals with intermediate composition have structures based on the ordered intergrowth of units of an end-member struc-

0003–004X/95/1112–1166$02.00

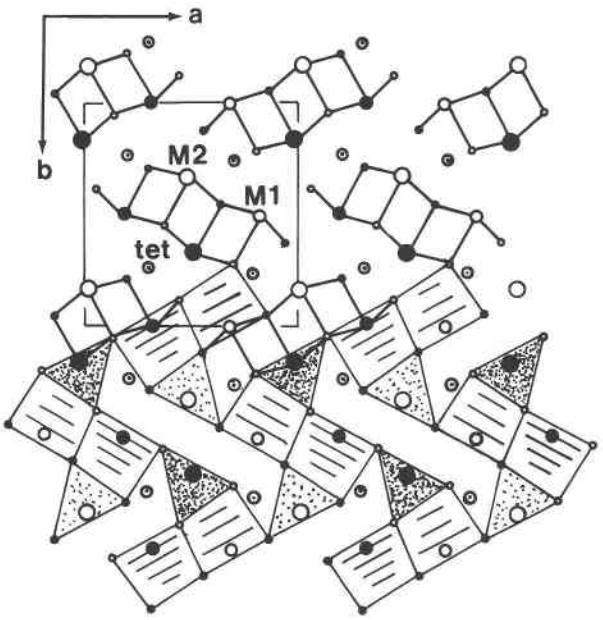


Fig. 1. Schematic diagram of the bismuthinite structure projected down [001] showing the location of vacant tetrahedral sites. In the top half of the diagram the structure is depicted as quadruple $Bi_4S_6$ units; in the lower part of the structure it is shown as trigonal prisms. The M1 and M2 sites are indicated, as are the vacant tetrahedral sites. In the other members of the series Pb is ordered onto the M2 site and Cu onto the tetrahedral sites. Circles: solid, $z = \frac{1}{4}$; open, $z = \frac{3}{4}$; large, Bi in M2 site; medium, Bi in M1 site; small, S; medium with dot, vacant tetrahedral sites for Cu.

ture with units of the mid-member structure. The structure of hammarite, $Cu_2Pb_2Bi_4S_9$, is not a simple intergrowth of one aikinite cell with two krupkaite cells but rather consists of an ordered intergrowth of four krupkaite units with two aikinite units (4K + 2A) in space group *Pbnm,* forming a $3a$ supercell (Horiuchi and Wuensch, 1976) (Fig. 2). Structural and compositional data for the members of the bismuthinite-aikinite minerals are summarized in Table 1. [See Makovicky (1981) for a review of the crystallography of these minerals.]

In contrast to the highly ordered superstructures, extensive compositional fields have been reported in natural specimens from a variety of localities. Harris and Chen (1976) reported a compositional field of $Cu_{2-x}Pb_{2-x}Bi_{2+x}S_6$ ($0.0 \leq x \leq 0.34$) for aikinite and $Cu_{1-x}Pb_{1-x}Bi_{3+x}S_6$ ($-0.13 \leq x \leq 0.34$) for krupkaite, whereas Mozgova et al. (1990) examined the composition of bismuthinite-aikinite minerals from the Inkur tungsten deposit, Transbaikal, Russia, and found less extensive compositional fields. Studies of synthetic samples by Springer (1971), Mumme and Watts (1976), and Chang and Hoda (1977) revealed complete structural solid solution between bismuthinite and aikinite above 300 °C, and all attempts to prepare the ordered superstructures have been unsuccessful. HRTEM studies showed that compositional variation in these minerals, from some deposits at least, is

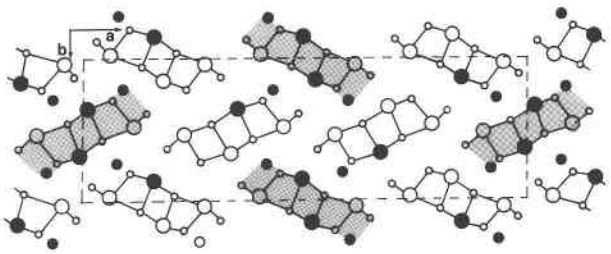


Fig. 2. Schematic diagram of the hammarite structure projected down [001] showing the ordering of the 2A units with 4K units in the unit cell. The two aikinite-like units are shaded.

due to the stacking disorder of the compositionally ordered structural strips (polysomatic strips) rather than simple random substitutional solid solution (Pring, 1989). In general, for any composition in the bismuthinite-aikinite series (that is, a mineral with the formula $Cu_xPb_x$-$Bi_{2-x}S_3$), there are three or four possible structural states: (1) complete solid solution, in which Pb is randomly substituted for Bi in the M2 site, and Cu is disordered over the available tetrahedral sites; (2) ordering of the Pb + Cu substitution into A, K, or B polysomatic strips and the disordered intergrowth of these strips; (3) disordered intergrowth of A, K, or B polysomatic strips with ordered strips of the higher (or supercell) members of the series, such as slabs of hammarite within a krupkaite matrix; and (4) fully ordered intergrowth of polysomatic strips, such as in hammarite (4K + 2A), when the composition matches that of a supercell member.

In 1989, long-term annealing experiments were initiated to follow the process of cation ordering in these minerals and to prepare well-ordered superlattice phases. The experiments were terminated in April 1994, at which time some samples had been annealed for 56 months. The hammarite composition was selected to represent the bismuthinite-aikinite series as a whole. Given the close relationship among members of the group, it seems reasonable that these experiments apply in general terms to the whole series.

## Experimental methods

A 20 g batch of synthetic hammarite, $Cu_2Pb_2Bi_4S_9$, was prepared by reacting stoichiometric proportions of $Cu_2S$,

**Table 1.** Minerals in the bismuthinite-aikinite series

| Mineral | Composition | *a* (Å) | *b* (Å) | *c* (Å) | Space group | Structure* |
|---|---|---|---|---|---|---|
| Bismuthinite | $Bi_2S_3$ | 11.23 | 11.27 | 3.91 | *Pbnm* | 2B |
| Pekoite | $CuPbBi_{11}S_{18}$ | 33.50 | 11.32 | 3.99 | *Pb2₁m* | 4B + 2K |
| Gladite | $CuPbBi_5S_9$ | 33.53 | 11.49 | 4.00 | *Pbnm* | 2B + 4K |
| Krupkaite | $CuPbBi_3S_6$ | 11.15 | 11.51 | 4.01 | *Pb2₁m* | 2K |
| Lindströmite | $Cu_3Pb_3Bi_7S_{15}$ | 56.11 | 11.57 | 4.00 | *Pbnm* | 8K + 2A |
| Hammarite | $Cu_2Pb_2Bi_4S_9$ | 33.77 | 11.59 | 4.01 | *Pbnm* | 4K + 2A |
| Friedrichite | $Cu_5Pb_5Bi_7S_{18}$ | 33.84 | 11.65 | 4.01 | *Pb2₁m* | 2K + 4A |
| Aikinite | $CuPbBiS_3$ | 11.32 | 11.64 | 4.01 | *Pbnm* | 2A |

* B = bismuthinite units, K = krupkaite units, A = aikinite units.

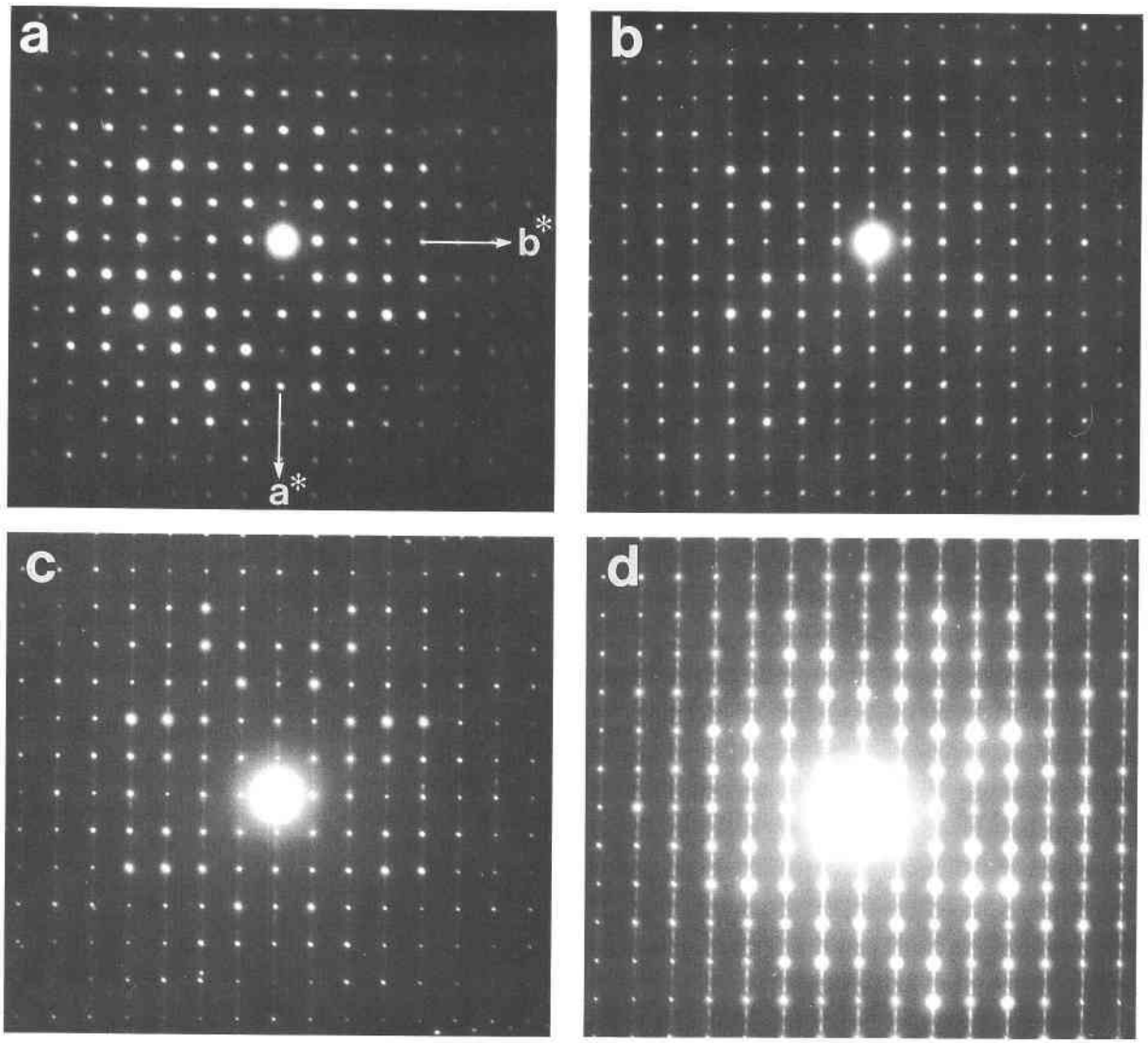


Fig. 3. Electron diffraction patterns for synthetic hammarite annealed at 175 °C for (**a**) four months, (**b**) 12 months, (**c**) 20 months, and (**d**) 32 months. Note the absence of superlattice reflections along **a*** after four months of annealing, whereas after 32 months the superlattice reflections are strong but not very sharp.

PbS, and $Bi_2S_3$ in a sealed, evacuated silica tube at 500 °C for 25 d. The sample was quenched, reground, and heated for an additional 25 d at 500 °C to obtain a more homogeneous product. The polycrystalline synthetic hammarite was divided into 24 charges, which were sealed in evacuated silica tubes. Twelve tubes were loaded into a muffle furnace and annealed at 175 ± 5 °C, while the other 12 samples were annealed in a similar furnace at 225 ± 5 °C. Pring (1989) suggested that the ordering temperatures may be about 200 °C on the basis of TEM observations, and the annealing temperatures were selected to be on either side of this value. The annealing experiments ran continuously (minor power outages excepted) for 56 months. A tube was removed from each furnace every four months for the first 40 months of the experiment, and the final two samples remained in the furnaces for 16 additional months. The furnaces were turned off briefly while the samples were removed to ensure that the furnace temperature did not exceed the annealing temperature. The extent of cation ordering and supercell formation was assessed by monitoring sharpness of supercell reflections by electron diffraction. Specimens were prepared for electron microscopy by grinding under acetone in an agate mortar, and the fracture fragments were dispersed from suspension onto Cu grids coated with holey carbon support films. The electron diffraction patterns were obtained using several electron microscopes but mainly a JEOL 2000 FX, operating at 200 kV and fitted with a side-entry ±60° double-tilt goniometer and an energy-dispersive X-ray analysis system (EDS). The large tilt range greatly facilitated the recording of several [001] diffraction patterns for each crushed sample. Diffraction

patterns were recorded from at least six crystal fragments in each of the 24 samples examined. High-resolution images were obtained for selected specimens to assess the extent and nature of compositional ordering, using a JEOL 200 CX transmission electron microscope fitted with a specially modified side-entry ±15° double-tilt goniometer. The limited tilt of this instrument made locating suitable crystal fragments difficult, and image data were obtained for only eight samples. The optical parameters for this instrument are $C_s = 0.41$, $C_c = 0.90$ Å, and at 200 kV the point-to-point resolution is 1.8 Å and the Scherzer defocus is −393 Å. Simulations of high-resolution images were performed by the conventional multislice method (Goodman and Moodie, 1974), using local programs based on the routines by G. R. Anstis (personal communication). Ordering schemes for the hammarite composition were derived from the atomic coordinates for the hammarite and gladite structures (Horiuchi and Wuensch, 1976; Kohatsu and Wuensch, 1976).

Attempts were made to monitor the compositions of the crystal fragments using the JEOL 2000 FX fitted with the EDS system; these experiments were not successful. Overlap of lines in the EDS spectra of these minerals is extensive, and the variations in X-ray line intensities owing to the size and shape of the crystal fragments were greater than those caused by the compositional differences among hammarite, krupkaite, lindströmite, and friedrichite.

## Results

Figure 3 shows a selection of [001] diffraction patterns for the hammarite samples annealed at 175 °C. The electron diffraction patterns reveal the progressive appearance of superlattice reflections along the $a^*$ direction. The samples annealed at 225 °C gave a similar set of results. The extent of supercell formation within individual samples varied considerably from grain to grain. The diffraction patterns in Figure 3 represent the most ordered state observed for each annealing period. In addition to the $3a$ superlattices, $5a$ superlattices were observed in samples annealed for periods of 24 months or longer, indicating some compositional variation within the products (Fig. 4). The $3a$ superlattice corresponds to hammarite, whereas the $5a$ superlattice could correspond to either $Cu_3Pb_3Bi_7S_{15}$ (lindströmite) or $Cu_7Pb_7B_{11}S_{30}$, a phase not known in nature but with a composition between hammarite and friedrichite. It was not possible to establish the composition with the EDS system fitted to the JEOL 2000 FX microscope. The progressive formation of chemically distinct structural slabs in the synthetic hammarite samples annealed at 175 and 225 °C is revealed by high-resolution lattice images (Fig. 5). The images indicate that cations first order on a local scale to create end-member polysome strips, which are unit-cell–wide strips of aikinite and krupkaite, and then these polysome strips themselves order to form supercells. In the intermediate state between solid solution and ordered supercell (Fig. 5a and 5c), the crystals consist of disordered

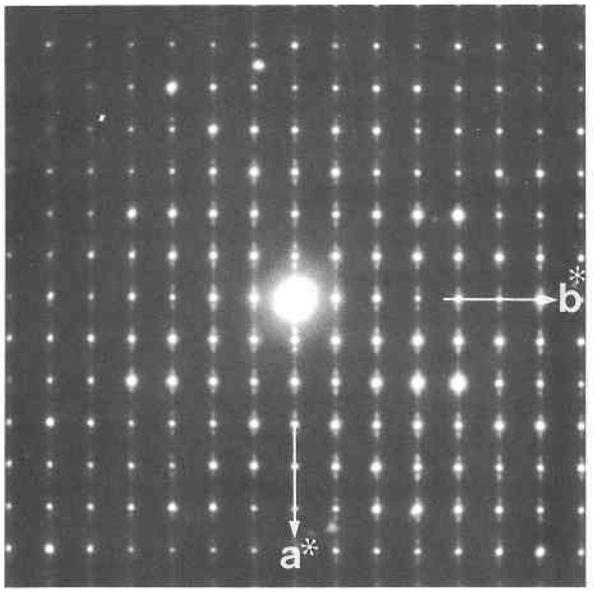


Fig. 4. Electron diffraction pattern for the $5a$ supercell phase from a sample of synthetic hammarite annealed at 225 °C for 24 months.

intergrowths (stacking disorder) of compositionally distinct slabs (Fig. 5b). The diffraction pattern corresponding to this image shows streaks rather than distinct satellite reflections.

Although the superlattice diffraction effects, continuous streaks and distinct satellite reflections (although somewhat streaked) (Fig. 3b–3d), are similar to those observed in natural members of the bismuthinite-aikinite series (Pring, 1989), they do not necessarily reflect the same structural states. The streaked diffraction patterns observed for natural specimens in the previous study were the result of disordered stacking along **a** of well-ordered structural slabs; very few breaks in continuity of cation ordering along **b** were observed. Such breaks in continuity appear as steps in the lattice rows (one such step is seen in Fig. 3d of Pring, 1989). The corresponding images in this study show many breaks in the correlation of the Pb + Cu ordering between cells along **b** and reveal a less ordered structural state (Fig. 5b).

## Discussion

There are few measurements of the mobility of $Pb^{2+}$ and $Cu^+$ in sulfides; however, on the basis of phase-transition data for copper sulfides, it is clear that $Cu^+$ is quite mobile at the annealing temperatures used in these experiments (Putnis, 1977). The larger radius of $Pb^{2+}$ might cause a lower mobility relative to $Cu^+$, and the ordering of $Pb^{2+}$ on the M2 site may be the rate-determining step in the overall cation-ordering process in these structures. It is also possible that the diffusion of $Cu^+$ and $Pb^{2+}$ is coupled. Determination of the ordering process depends on the starting state of the synthetic hammarite. A crucial question is whether all the $Pb^{2+}$ initially is disordered

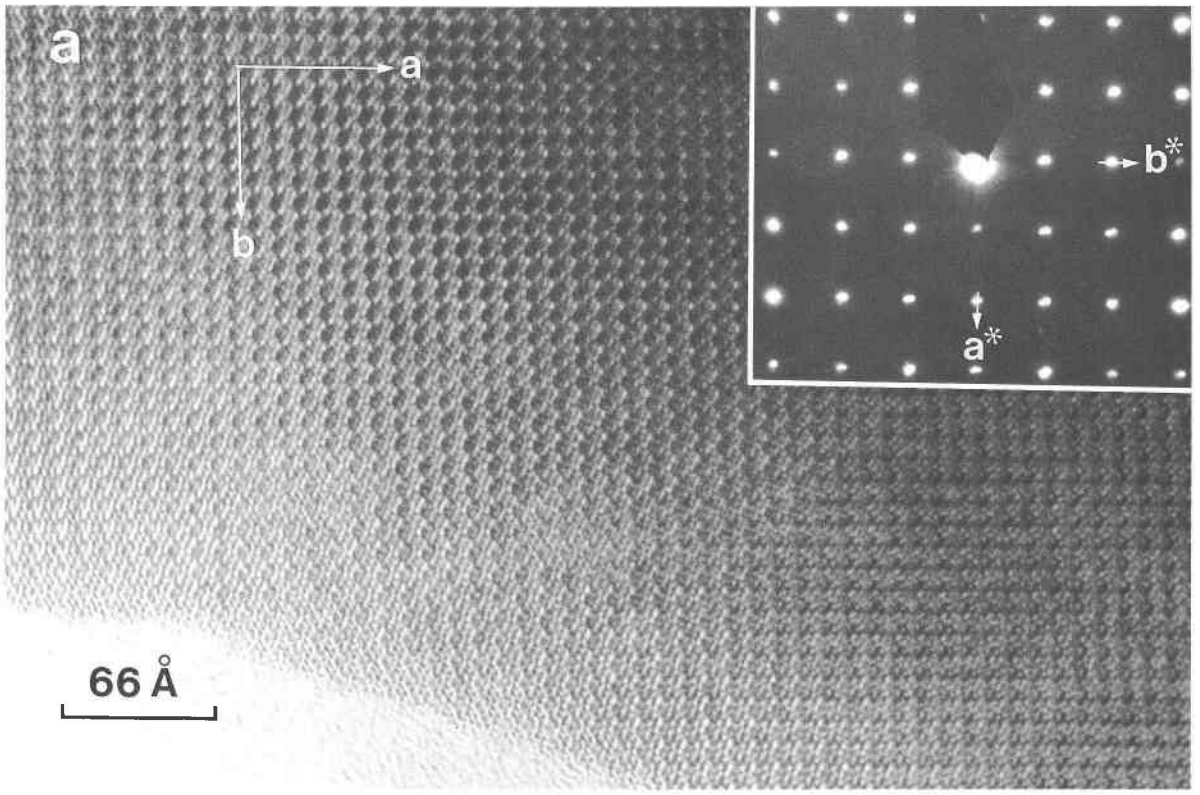
a
a
b
b*
a*
66 Å

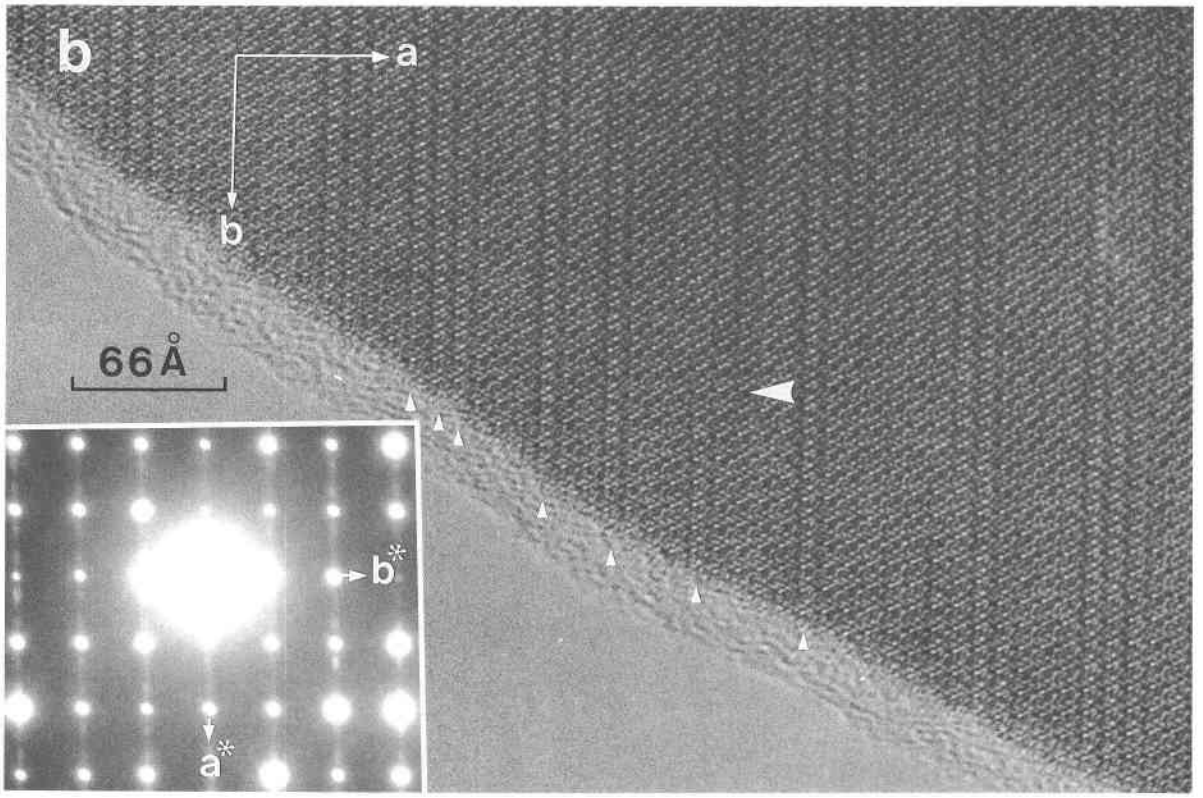
b
a
b
66 Å
b*
a*

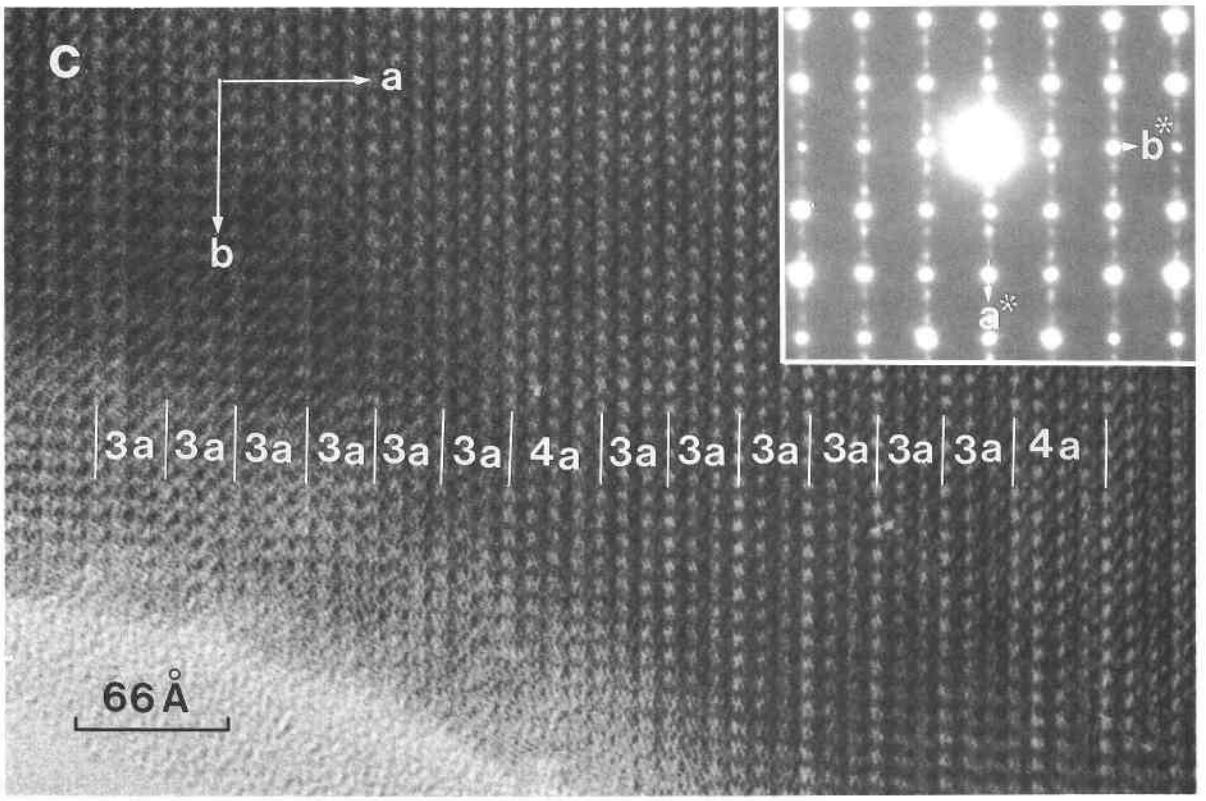


Fig. 5 (left and above). Lattice images and corresponding electron diffraction patterns for synthetic hammarite annealed at 175 and 225 °C. (**a**) After four months at 175 °C, showing no evidence of cation ordering. (**b**) After 32 months at 175 °C, showing the formation of compositionally ordered strips with poor correlation along **b** and disorder along **a**. The individual aikinite strips are indicated with small arrowheads. The large arrowhead indicates a break in the ordering. (**c**) After 56 months at 225 °C, showing well-developed, compositionally distinct slabs of 3*a* and 4*a* supercells.

only on the M2 site or over both the M1 and M2 sites. Horiuchi and Wuensch (1976) showed that in hammarite all the Pb is ordered on the M2 site of the bismuthinite parent and that two sites (M1 and M2) are crystal-chemically distinct. Mumme and Watts (1976) refined the cation distribution in pekoite (the 4B + 2K superstructure) using superlattice reflection intensity data and assigned all the $Pb^{2+}$ to the M2 site. They found that this site was displaced 0.5 Å from its ideal position in the bismuthinite structure. Mumme and Watts (1976) also investigated the nature of the ordering processes by single-crystal X-ray diffraction methods using synthetic crystals grown by $I_2$ vapor-transport methods at 500 °C. Although they discerned no superlattice reflections in their X-ray photographs, they found, on the basis of bond-length data, that $Pb^{2+}$ was ordered on the M2 site rather than the M1 site. Thus, it seems probable that the initial structural state of the hammarite is the archetype cell in which $Cu^{+}$ is disordered over the four tetrahedral sites, $Pb^{2+}$ and $Bi^{3+}$ are disordered over the M2 site, and $Bi^{3+}$ occupies the M1 site.

Ordering of Pb over eight of the 12 available M2 positions in the supercell should produce some intensity in some of the hammarite superlattice reflections because this process is associated with displacements in these positions. In their structure refinement of gladite, Kohatsu and Wuensch (1976) found that displacements of the M2 site associated with Pb ordering was the principal contribution to superlattice intensity. However, because $Pb^{2+}$ and $Bi^{3+}$ are isoelectronic and the displacements are small, this ordering does not produce noticeable changes in image contrast at crystal thicknesses that permit valid use of the multislice method (<100 Å). Therefore, it is not possible to follow the process of ordering of Pb and Bi with HRTEM; however, the ordering of $Cu^{+}$, which is ordered over otherwise vacant sites, can be seen. This is illustrated by the series of image simulations shown in Figure 6. It should be noted that because of the nature of the fracture in these minerals, in general the crystal fragments examined in this study were considerably thicker than 100 Å, and no attempt was made to obtain detailed image matching using the multislice method.

If $Pb^{2+}$ ordering is independent of $Cu^{+}$ ordering, then one may expect to find superlattice intensity in the electron diffraction pattern but no noticeable contrast changes in the images. The images show considerable changes in

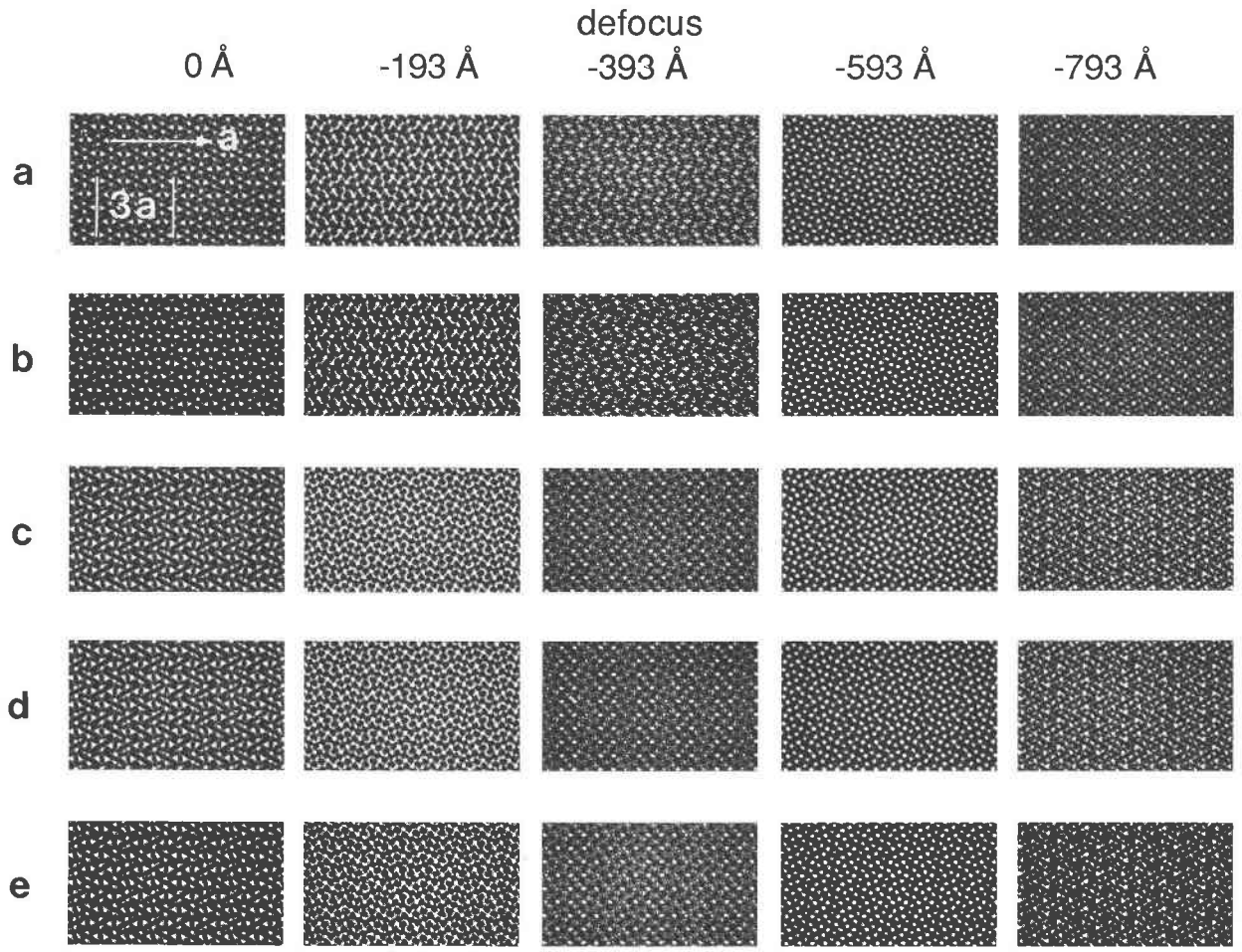


Fig. 6. Through-focal series of image simulations of the possible ordering states of the hammarite composition. The instrument parameters for the simulations are 200 kV, $C_s$ = 0.41 mm, foil thickness 100.25 Å. (a) Solid solution Pb and Bi disordered over the M2 sites and Cu disordered over the available tetrahedral sites. (b) Pb and Bi ordered over the M2 sites and Cu disordered over the available tetrahedral sites. (c) Pb and Bi disordered over the M2 sites and Cu ordered over the tetrahedral sites. (d) Fully ordered hammarite. (e) A 3*a* supercell based on one aikinite cell and two krupkaite cells.

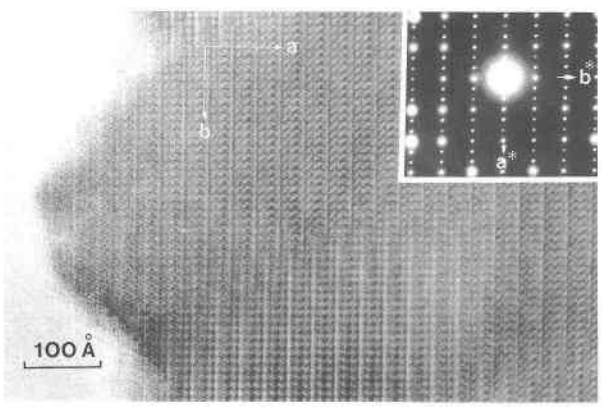


Fig. 7. Lattice image and corresponding electron diffraction pattern for hammarite from Gladhammar, Sweden, showing a distinctive 16.9 Å spacing. (For specimen and experimental details, see Pring and Hyde, 1987.)

contrast associated with the presence of superlattice reflections, and this suggests that ordering of $Cu^+$ and $Pb^{2+}$ is coupled.

It is evident when comparing the lattice image of ordered hammarite (Fig. 5c) and the hammarite image simulations (Fig. 6d) that they do not correspond well; the ordered hammarite simulations have a 16.9 Å repeat (1.5*a*) because of the centric distribution of A units in the cell rather than the 33.8 Å (3*a*) repeat shown in Figure 5c. Images of natural hammarite show the 16.9 Å repeat (1.5*a*) in thin regions, and the image detail matches well with the image simulations (Fig. 7). The 3*a* supercell observed in the annealed crystal has a different ordering scheme than that reported for natural hammarite; the structure appears to consist of a supercell based on the simple ordered intergrowth of one aikinite cell with two krupkaite cells, as shown in Figure 8.

It appears from electron diffraction and image data that

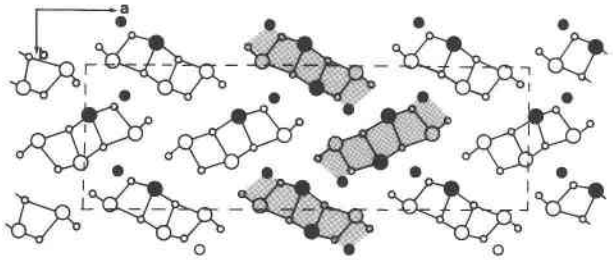


Fig. 8. Schematic diagram of a $3a$ supercell based on one aikinite cell and two krupkaite cells projected down [001]. The aikinite units are shaded.

ordering in synthetic hammarite proceeds through the following states: (1) solid solution with $Pb^{2+}$ and $Bi^{3+}$ disordered over the M2 sites and with $Cu^{+}$ disordered over the tetrahedral sites; (2) formation of A and K strips one unit cell wide, which show steps or breaks in continuity of $Pb^{2+}$-$Bi^{3+}$ and $Cu^{+}$ ordering along **a** and **b**; (3) formation of continuous A and K strips along **b** but with the disordered intergrowth of these strips along **a**; (4) formation of a simple supercell based on the ordered intergrowth of A and K cells; and (5) reordering of Pb-Bi and Cu cations into the higher symmetry hammarite supercell.

Given the long annealing times used in this experiment, it would not be feasible to monitor $Cu^{+}$ and $Pb^{2+}$ by single-crystal X-ray structure refinement methods. A more fruitful route may be to follow the disordering reaction by annealing well-ordered natural crystals of hammarite above the ordering temperature. The ordering temperature of the bismuthinite-aikinite intermediates is not yet established; the evidence of earlier phase studies and the annealing experiments reported here suggest that this temperature is between 225 and 300 °C. However, given that the longest period used in the previous annealing experiments was three months at 300 °C, and that it took 24 months of annealing at 225 °C before the extent of partial ordering was sufficiently advanced to be detected by electron diffraction, the ordering temperature could be above 300 °C.

Nevertheless, it is clear that under the geological conditions at which these minerals form, true structural solid solution in these minerals would occur only at very rapid cooling rates. One would expect nearly all natural material to consist of compositionally well-ordered strips, which, depending on the initial composition and the cooling rate, would be disordered intergrowths or ordered superstructures.

## Acknowledgments

I wish to thank D.A. Jefferson of the University Chemical Laboratories of the University of Cambridge and O. Greis of the University of Hamburg-Harburg for providing access to the electron microscope facilities in their charge. I also wish to thank Armin Reller for his hospitality at the University of Hamburg. The manuscript benefited from the helpful suggestions of the two referees, P.J. Heaney and K. Sickafus, and of G.D. Guthrie. I also thank P. Self of CSIRO Division of Soils for his help with image interpretation. The financial assistance of the Alexander von Humboldt Foundation and the Australian Research Council is gratefully acknowledged.

## References cited

Chang, L.L.Y., and Hoda, S.H. (1977) Phase relations in the system PbS-$Cu_2S$-$Bi_2S_3$ and the stability of galenobismutite. American Mineralogist, 62, 346–350.

Goodman, P., and Moodie, A.F. (1974) Numerical evaluation of N-beam wave functions in electron scattering by the multi-slice method. Acta Crystallographica, A30, 280–290.

Harris, D.C., and Chen, T.T. (1976) Crystal chemistry and re-examination of nomenclature of sulfosalts in the aikinite-bismuthinite series. Canadian Mineralogist, 14, 194–205.

Horiuchi, H., and Wuensch, B.J. (1976) The ordering scheme for metal atoms in the crystal structure of hammarite, $Cu_2Pb_2Bi_4S_9$. Canadian Mineralogist, 14, 536–539.

Kohatsu, I., and Wuensch, B.J. (1971) The crystal structure of aikinite $PbCuBiS_3$. Acta Crystallographica, B27, 1245–1252.

——— (1976) The crystal structure of gladite $PbCuBi_5S_9$, a superstructure intermediate in the series $Bi_2S_3$-$PbCuBiS_3$ (bismuthinite-aikinite). Acta Crystallographica, B32, 2401–2409.

Makovicky, E. (1981) The building principles and classification of bismuth-lead sulphosalts and related compounds. Fortschritte der Mineralogie, 59, 137–199.

Mozgova, N.N., Nenasheva, S.N., Chistyakova, N.I., Mogilevkin, S.B., and Sivtsov, A.V. (1990) Compositional fields of minerals in the bismuthinite-aikinite series. Neues Jahrbuch für Mineralogie Monatshefte, 35–45.

Mumme, W.G. (1975) The crystal structure of krupkaite, $CuPbBi_3S_6$, from the Juno Mine at Tennant Creek, Northern Territory, Australia. American Mineralogist, 60, 300–308.

Mumme, W.G., and Watts, J.A. (1976) Pekoite, $CuPbBi_{11}S_{18}$, a new member of the bismuthinite-aikinite mineral series: Its crystal structure and relationship with naturally and synthetically formed members. Canadian Mineralogist, 14, 322–333.

Ohmasa, M., and Nowacki, W. (1970) A re-determination of the crystal structure of aikinite $[BiS_2|S|Cu^{IV}Pb^{VII}]$. Zeitschrift für Kristallographie, 132, 71–86.

Pring, A. (1989) Structural disorder in aikinite and krupkaite. American Mineralogist, 74, 250–255.

Pring, A., and Hyde, B.G. (1987) Structural disorder in lindstromite: A bismuthinite-aikinite derivative. Canadian Mineralogist, 25, 393–399.

Putnis, A. (1977) Electron diffraction study of phase transformations in copper sulfides. American Mineralogist, 62, 107–114.

Springer, G. (1971) The synthetic solid-solution series $Bi_2S_3$-$BiCuPbS_3$ (bismuthinite-aikinite). Neues Jahrbuch für Mineralogie Monatshefte, 440–448.

Manuscript received July 19, 1994
Manuscript accepted June 22, 1995